Energy & Environmental Science

Accepted Manuscript

This article can be cited before page numbers have been issued, to do this please use: L. Nazar, M. Cuisinier, P. Cabelguen, B. Adams, A. Garsuch and M. Balasubramanian, *Energy Environ. Sci.*, 2014, DOI: 10.1039/C4EE00372A.




ROYAL SOCIETY OF CHEMISTRY

www.rsc.org/ees

View Article Online
DOI: 10.1039/C4EE00372A

Energy & Environmental Science

RSCPublishing

ARTICLE

# Unique Behaviour of Nonsolvents for Polysulphides in Lithium-Sulphur Batteries.

Cite this: DOI: 10.1039/xoxxoooooox

M. Cuisinier [a], P.-E. Cabelguen [a], B. D. Adams [a], A. Garsuch [b], M. Balasubramanian [c] and L. F. Nazar [a,*]

Received 30th January 2014,
Accepted 28th April 2014

DOI: 10.1039/xoxxoooooox

www.rsc.org/

Combination of a solvent:salt complex [Acetonitrile$(ACN)_2$:LiTFSI] with a highly fluorinated ether (HFE) co-solvent unveil a new class of Li-S battery electrolytes. They possess stability against Li metal and viscosities which approach that of conventional ethers, but have the benefit of low volatility and minimal solubility for lithium polysulphides while exhibiting an uncharacteristic sloping voltage profile. In the optimal system, cells can be discharged to full theoretical capacity under quasi-equilibrium conditions while sustaining high reversible capacities (1300-1400 mAh $g^{-1}$) at moderate rates, and capacities of 1000 mAh $g^{-1}$ with almost no capacity fade at fast discharge rates under selected cycling protocols. A combination of *operando* X-ray absorption spectroscopy at the S K-edge, and electrochemical studies demonstrate that lithium polysulphides are indeed formed in these ACN-complexed systems. Their limited dissolution and mobility in the electrolyte strongly affect the speciation and polysulphide equilibria, leading to controlled precipitation of $Li_2S$.

**Broader context.**

Markets for energy storage that go beyond portable electronics have rapidly emerged this decade, including powering electric vehicles and storage of electricity from renewable sources. These require a step change in energy density that is unlikely to be met by conventional Li-ion batteries, where estimates suggest they are reaching theoretical energy density limits. But in the world of "beyond lithium-ion", the options are limited. One of the most hopeful is lithium-sulphur (Li-S) batteries, which are receiving tremendous attention. These future generation systems that use elemental sulphur offer up to 3-fold increased energy densities and greatly reduced cost factors, but commercial use is so far hindered by several challenges. In particular, these include poor Coulombic efficiency and capacity fading due to the dissolution of polysulphide intermediates in the electrolyte. In this work, we take a different approach to the Li-S battery by developing new binary electrolyte systems based on solvent-salt complexes that possess no solubility for the lithium polysulphide, enabling full theoretical capacity to be achieved. Fundamental investigations reveal details of the underlying mechanism of the redox chemistry. This also renders physical confinement unnecessary, so that at moderate to fast discharge rates, high reversible capacities can be delivered with minimal capacity fade with a commercial carbon black. This approach shows the way forward to increase the electrode sulphur loading by developing electrode architectures with tailored porosity without risk of polysulphide dissolution.

## Introduction

The reality of ever increasing $CO_2$ emissions from combustion of hydrocarbons and coal and its consequences in environmental and economic spheres, along with dramatically increasing urban pollution in rapidly growing economies, make the development of improved electrochemical energy storage systems critical for a better future. In this context, the moderate but yet unsatisfactory energy density of Li-ion batteries, and their high materials cost hampers their spread to more demanding applications such as automotive transport and renewable energy storage. Lithium batteries based on elemental sulphur are one of the promising candidates as a successor to insertion-based Li-ion technology. Sulphur is exceedingly abundant, inexpensive, and exhibits a high theoretical specific capacity and energy of 1672 mAh $g^{-1}$ and 2600 Wh $kg^{-1}$ based on the assimilation reaction: $S_8 + 16Li \leftrightarrow 8Li_2S$[1,2]. The volumetric energy density is more difficult to calculate in the absence of commercial cell production, but the assumption of a low volume-electrolyte cell leads to theoretical values of 2800 Wh $L^{-1}$, and practical values of 750 Wh $L^{-1}$ in the presence of a protected lithium negative electrode that requires little lithium excess[3]. However, there are numerous problems with practical Li-S cells that arise from a complex discharge process during which multiple redox equilibria occur. Lithium polysulphide intermediate species $Li_2S_n$ ($2 \leq n \leq 8$)[4] readily dissolve into the polar organic solvents commonly used in electrolytes[5]. Their migration to and from the negative electrode creates a redox "shuttle" phenomenon that can lead to poor coulombic efficiency, loss of active material from the positive electrode on

View Article Online
Energy & Environmental Science
DOI: 10.1039/C4EE00972A



repeated cycling, and impedance build-up on the electrode surfaces[6]. Although protection of the lithium metal may prevent problems at the negative electrode[7,8], these issues are still a concern at the positive electrode. On the other hand, electrochemical reactions that occur in solution offer the advantage of much faster kinetics compared to the solid state, especially when the solid products exhibit ultra-low electronic and ionic conductivities, which is the case for both sulphur and $Li_2S$.[3]

Therefore, the design of an optimized electrolyte solvent or solvent blend for the Li-S system is essential. In addition to the constraint that the electrolyte meet certain critical properties (a wide voltage window, and sufficient $Li^+$ conductivity to ensure satisfactory rate capability), it has to exhibit specific requirements for Li-S batteries such as stability with respect to chemical attack from $Li_2S_n$ species that are formed upon discharge[9,10]. The importance of the solvation ability of polysulphides is still unclear, however. With lithium bis(trifluoromethanesulfonyl)imide (LiTFSI) as the most common salt, 1, 2-dimethoxy ethane (DME), and other ethylene glycol ethers are the electrolyte of choice in Li-S batteries where they are usually paired with 1, 3 dioxolane (DOL), owing to its low viscosity and SEI-forming properties[11,12,13]. However, these organic solvents greatly suffer from their high volatility which limit their practical use. Thus, room-temperature ionic liquids (RTILs), consisting of coordinated cations and anions, are of high interest owing to their high stability, nonflammability and nonvolatility. In the particular case of Li-S batteries, they could help to tune the solubility and mobility of $Li_2S_n$ due to their unique complexed configuration, as demonstrated by Song *et al.*[14]. Recently, glyme-Li equimolar complexes proved to exhibit a RTIL-like behavior[15]. Indeed, the glyme structure is favourable for the solvation of lithium ion due to the presence of solvating oxygen atoms, which acts as Lewis basis that dissociates lithium salts, especially in the case of long chains such as in tetra(ethylene glycol)-dimethyl ether (TEGDME)[16]. These electrolytes showed promising results for the Li-S system[17,18,19], especially in terms of coulombic efficiency. This has been explained by the suppression of the redox shuttle by minimizing $Li_2S_n$ solubility in the electrolyte, similarly to other RTILs[20].

Here, we report on the interesting new perspectives offered by a specific $(acetonitrile)_2$:LiTFSI complex[21,22] for Li-S batteries. Since all of the acetonitrile molecules are effectively bound by formation of the 2:1 complex[21], not only is their reaction with metallic lithium prevented[22], but we show that the electrolyte solubility for polysulphides is suppressed. To lower the viscosity, we blend $(ACN)_2$:LiTFSI with 1,1,2,2-tetrafluoroethyl 2,2,3,3-tetrafluoropropyl ether (HFE). A similar concept was recently reported by Dokko *et al.* for glyme-based RTILs.[23] The HFE is too fluorinated to participate in $Li^+$ solvation[23,24], and therefore in the case of the glymes, including dimethoxyethane[24], HFE also serves to minimize polysulphide solubility. Such extra precaution is not needed for $(ACN)_2$:LiTFSI, whose unique nonsolvent character *vis a vis* polysulphides unveils a distinctive sulphur electrochemistry. Our approach to optimize the [$(ACN)_2$:LiTFSI]:HFE volume ratio is based on consideration of the physical parameters balanced with the electrochemical properties in terms of sulphur utilization, impedance, polarization and capacity retention in a Li-S cell. This is summarized in **Scheme 1**. Most importantly, our investigation of the atypical and unique Li-S voltage profile by both *operando* X-ray absorption spectroscopy (XANES) and classical electrochemical methods sheds much light on the underlying redox process in this complex media. We demonstrate that lithium polysulphides are formed in ACN-complexed electrolytes despite their almost negligible solubility, but they exhibit extremely limited mobility which significantly affects sulphur speciation in the cell, and thereby the overall electrochemical behaviour.

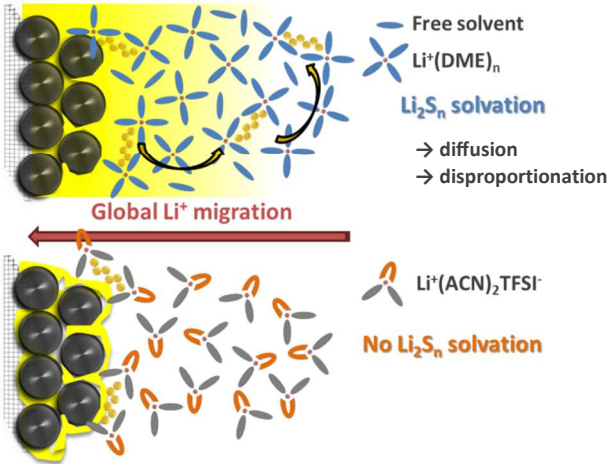


**Scheme 1.** Concept of a nonsolvent for polysulphides in a Li-S battery.

## Experimental details

**Preparation of the CMK-3/S material and electrodes.**
In order to rule out limitations due to poor electronic conduction and volume expansion, "standard electrodes" were based on a 50 wt% sulphur CMK-3/S nanocomposite prepared by melt-diffusion, as reported elsewhere[25]. Positive electrodes were cast from a slurry containing 80 wt% CMK-3/S composite, 10 wt% Super-S carbon and 10 wt% poly(vinylidene fluoride-co-hexafluoropropene) binder in N,N-dimethylformamide onto a carbon-coated aluminum current collector (Intelicoat). Sulphur loading was fixed to 1 mg $cm^{-2}$.

**Preparation and source for the electrolytes**
The reference electrolyte, provided by BASF, was composed of 1 M bis(trifluoromethane-sulfonyl)imide lithium (LiTFSI) in a mixed solvent of 1,2-dimethoxyethane (DME) and 1,3-dioxolane (DOL) (v/v = 1:1), with 2 wt % of lithium nitrate ($LiNO_3$). Other electrolytes were home made from dried LiTFSI (BASF) and either tetraethylene glycol dimethyl ether (TEGDME, Sigma Aldrich), ethyl methyl sulfone (EMS, abcr), or acetonitrile (ACN, Sigma Aldrich). 1,1,2,2-tetrafluoroethyl 2,2,3,3-tetrafluoropropyl ether (HFE) was purchased from Synquest Labs.

**Characterization of electrolyte solutions**
The viscosity was measured using a μVISC viscometer (Rheosense) and the appropriate chip (0-100 mPa s or 100-20000 mPa s) and the ionic conductivity with a 3-star conductimeter (Orion) equipped with a 2-electrode epoxy conductivity probe (cell constant of 1.0 $cm^{-1}$). Thermo-gravimetric analysis (TGA) was carried out under air using a TA instrument SDT Q600. The temperature was increased to 70°C and held for 180 min to evaluate the electrolyte volatility.

**Electrochemistry**
Coin cells (2325, NRC) were fabricated in an argon-filled glovebox using a sulphur electrode, two sheets of 3501 CelgardTM as the separator, a Li foil negative electrode, and 50 μL of electrolyte. For galvanostatic tests at 20°C, the cut-off

Energy & Environmental Science
View Article Online
DOI: 10.1039/C4EE00372A
ARTICLE



voltage was 1.85 V in the presence of $LiNO_3$ or 1.2 V otherwise (Arbin instrument). Electrochemical Impedance Spectroscopy (EIS) was measured at the open-circuit voltage (OCV) on a VMP-Z instrument (Bio-logic) between 200 kHz and 20 mHz. Similar instrument was used to perform galvanostatic intermittent titrations (GITT), by alternating C/10 pulses (20 min) with OCV periods (60 min). A discharge/charge rate of 1C corresponds to a full discharge in one hour, i.e. a current of 1672 mA $g^{-1}$. For potential staircase voltammetry, steps were set to 5 mV $h^{-1}$ with an additional C/50 or C/100 current limit on the step duration.

**XANES**

The experiments were carried out at the sector 9-BM-B in the Argonne National Laboratory using a Si(111) crystal monochromator. The instrumental resolution in the energy range near the sulphur K-edge is about 0.35 eV, with a beam size of about 450 x 450 µm. All of the XANES studies were carried out under constant helium flow in the sample chamber and the data were collected in fluorescence mode using a 4-element vortex detector. Energy calibration was carried out using sodium thiosulfate pentahydrate, with the pre-edge feature at 2469.2 eV. The cell used to perform *operando* XANES was adapted from the 2325 coin cells using an aluminized Kapton™ window[26]. Other modifications were limited to the electrode design: CMK-3/S -15wt% was mixed with Super P and PVDF to reach 10 wt% sulphur and cast onto a carbon paper (AvCarb P50, Ballard Material Products). Additional experimental considerations are given as Supporting Information.

## Results and discussion

### Physicochemical properties of $(ACN)_2$:LiTFSI compared to common Li-S electrolytes.

Molecular dynamic simulations combined with Raman spectroscopy suggest that the unique $(ACN)_2$:LiTFSI stoichiometry adopts a structure where all the solvent molecules, cations and anions are fully complexed[21], resulting in its unusual stability *vs.* metallic lithium[22]. The ionic conductivity and viscosity of this complex electrolyte (see **Table 1**) constitute the main parameters that impact the performance of this electrolyte, although the density and the thermal stability were also examined to evaluate its practical utilization. These metrics are reported along with the values measured for DOL:DME (1:1) – 1 M LiTFSI / 2 wt% $LiNO_3$; TEGDME – 1 M LiTFSI; and EMS – 1.2 M LiTFSI which are more common electrolytes for Li-S batteries (the concentration of LiTFSI is omitted in subsequent denotations). In good agreement with the literature, DOL:DME (1:1) offers the highest ionic conductivity of 10.8 mS $cm^{-1}$, whereas $(ACN)_2$:LiTFSI exhibits the lowest value of 1.35 mS $cm^{-1}$, not far below TEGDME and EMS based electrolytes (2.01 mS.$cm^{-1}$ and 2.25 mS $cm^{-1}$, respectively). As shown in **Table 1**, the viscosity of $(ACN)_2$:LiTFSI is one to two orders of magnitude higher than the other electrolytes commonly reported for Li-S. As explained by Seo *et al.*[21], this is because all the solvent molecules are coordinated to the $Li^+$ cations, and so no free ACN is available to act as a "lubricant" for solvated species. This results in increased stability at moderate temperature compared to the DOL:DME based electrolyte, which is essential for practical applications.

| Electrolyte | Ionic conductivity (mS.$cm^{-1}$) | Viscosity (cP) | Density (g.$cm^{-3}$) | Mass retention after 180 min at 70 °C (%) |
|---|---|---|---|---|
| **DOL:DME (1:1) – 1 M** | 10.8 | 2.2 | 1.07 | 68.7 |
| **TEGDME – 1 M** | 2.01 | 13.0 | 1.14 | 98.8 |
| **EMS – 1.2 M** | 2.25 | 23.3 | 1.30 | 99.5 |
| **$(ACN)_2$:LiTFSI – 3.7 M** | 1.35 | 138 | 1.34 | 87.9 |
| **ACN :HFE (1:1) – 1.8 M** | 1.57 | 8.6 | 1.47 | 90.4 |

**Table 1. Physicochemical parameters of selected nonaqueous electrolytes compared to $(ACN)_2$:LiTFSI.**

**Physicochemical properties of [$(ACN)_2$:LiTFSI]:HFE blends.** Previous Li-S studies show that high viscosities result in poor electrochemical performance, especially in terms of sulphur utilization[12]. To use $(ACN)_2$:LiTFSI in a Li-S cell, our strategy consisted of blending it with HFE to decrease its viscosity. Dokko *et al.* used a similar approach for the TEGDME:LiTFSI equimolar complex[23]. Regarding the transport properties, the combination of the low polarity of HFE and the steric hindrance of the chelating oxygen by fluorine completely suppress its ionic solvation properties. Because neither LiTFSI nor $Li_2S_6$ have solubility in this medium, values were too low to be titrated (see Supporting info, **Figure S1**). It makes HFE a solvent of choice in this work, because it preserves the unique characteristics of the acetonitrile-lithium salt complex. Upon HFE addition to $(ACN)_2$:LiTFSI, the trade-off between decreasing the viscosity (i.e. increasing $Li^+$ mobility) and over-diluting the concentration of charge carriers can be probed experimentally based on the variation of the molar ionic conductivity (see SI, **Figure S2**). A maximum of 0.86 mS $cm^{-1}$ $mol^{-1}$ was achieved with 50 vol% HFE so that intermediate formulations with 50 vol% or 66 vol% HFE exhibit both a reasonable compromise between viscosity and ionic conductivity (see **Table 1**). The values are comparable to TEGDME or EMS based electrolytes, while the ACN:HFE mixtures offer virtually no solubility for lithium polysulphides.

To confirm the positive impact of HFE addition in a Li-S cell, electrochemical impedance spectroscopy (EIS) was performed at open circuit voltage (OCV) on full cells containing either pure $(ACN)_2$:LiTFSI or ACN:HFE blends– denoted simply as ACN:HFE (1:2); ACN:HFE (1:1); or ACN:HFE (2:1) in the following – as electrolytes (see SI, **Figure S3**). The positive impact of the HFE addition in Li-S cells is reflected by a progressive decrease of charge-transfer resistance – from ACN:HFE (2:1) to ACN:HFE (1:1), and ACN:HFE (1:2), respectively. This is assigned to improved wetting of the sulphur positive electrode with the decrease in viscosity. While 1,3-dioxolane fulfils this role in typical Li-S batteries, it also has very high solubility for polysulphides, whereas HFE has none (**Figure S1**). As a result, the ACN:HFE electrolyte formulations described here, while competing with the various glyme:DOL blends in terms of physico-chemical indicators, show very different electrochemical behavior in lithium-sulphur cells, behaving as nonsolvents.

**Behavior of [$(ACN)_2$:LiTFSI]:HFE electrolytes in Li-S cells.**

The electrochemical performance of Li-S cells that incorporate $(ACN)_2$:LiTFSI , ACN:HFE (1:1) and ACN:HFE (1:2) were compared to DOL:DME (1:1) by galvanostatic cycling. **Figure 1a** displays the voltage profiles of the first galvanostatic cycle while **Figure 1c** shows the capacity retention over 100 cycles at C/5 (i.e. 334 mA $g^{-1}$). For the "reference" cell containing DOL:DME (1:1), the discharge capacity of the first cycle was 1178 mAh.$g^{-1}$, in good agreement

View Article Online
Energy & Environmental Science
DOI: 10.1039/C4EE00372A



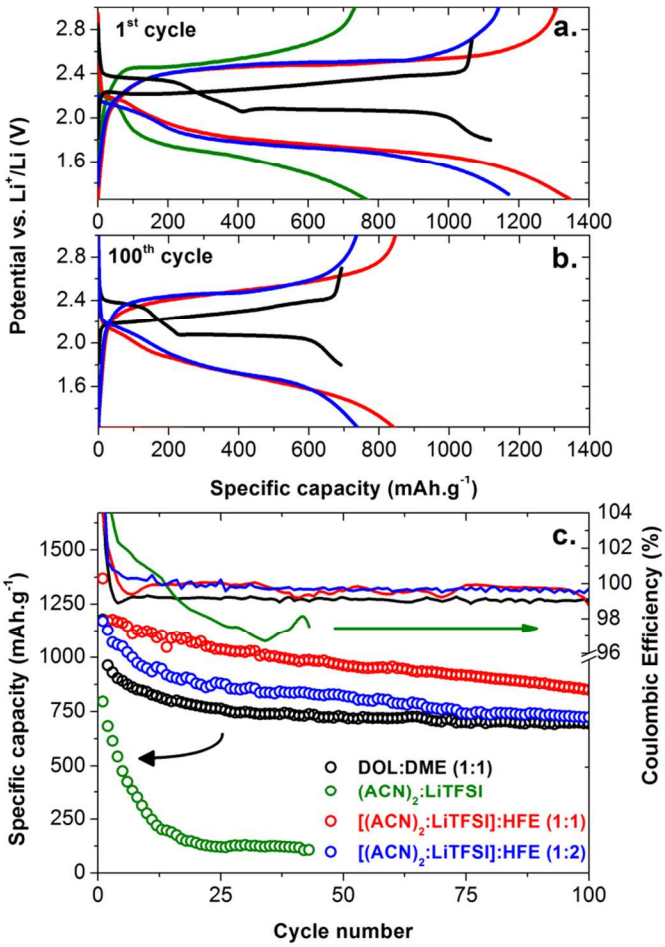


**Figure 1**. Galvanostatic cycling at C/5, comparison between DOL:DME (black), pure $(ACN)_2$:LiTFSI (green), ACN:HFE(1:1) (red) and ACN:HFE(1:2) (blue). **a.** Voltage profile of the first cycle and **b.** 100th cycle. **c.** Specific discharge capacity over 100 cycles. Coulombic efficiency is given in each case; note that only DOL:DME contains $LiNO_3$.

with values commonly reported in the literature[25]. The electrochemical signature is also very typical, consisting - during discharge - of two plateaus around 2.35 V and 2.1 V separated by a supersaturation point. It is generally accepted that the first reduction plateau corresponds to the conversion of $\alpha$-$S_8$ to soluble long-chain polysulphides while the second plateau is the signature of the reduction of polysulphides to insoluble $Li_2S$. Therefore, the two, 2-phase transitions, (i.e, solid → solution and then solution → solid) are well reflected in the two-step voltage profile[1,2]. The irreversible capacity below 1.9 V is attributed to the reduction of the $LiNO_3$ additive on the positive electrode[27]. The charge consists of a sloping curve terminated by a plateau at 2.4 V, which reflects the oxidation of $Li_2S$ to soluble polysulphides, and then to elemental sulphur[26].

In contrast, for $(ACN)_2$:LiTFSI, no supersaturation point, no overpotential and less clearly defined plateaus are observed. This is correlated to the structure of the electrolyte, in which solvate species are present as contact ion pairs (CIP) and aggregates[21] (AGG) rather than solvent separated ion pairs (SSIP) like in glyme:LiTFSI[16]. In the latter case, we believe the persistence of two distinct plateaux and a supersaturation "knee"[17,23] are consequences of the fast exchange rate between complexed and free glyme molecules. This would allow the solvation of lithium polysulphides upon cycling, despite saturation experiments on static solutions suggesting otherwise[23]. The moderate reversible capacity of 796 mAh $g^{-1}$, which decreases to 100 mAh $g^{-1}$ after 20 cycles (**Figure 1c**) is probably a direct consequence of the high viscosity of the electrolyte, as reported by others for TEGDME[12]. Also, the 0.8 V polarization (*vs.* 0.15 V in DOL:DME (1:1)) forces the voltage window to be extended down to 1.2 V; indicating that this electrolyte alone is not optimal for practical Li-S cells. This limitation can be overcome with a viscosity lowering co-solvent as we show below. Moreover, zero redox shuttle is observed as reflected by the Coulombic efficiency, indicating a very limited mobility for linear polysulphides as expected.

The fine-tuning of the physico-chemical properties by addition of HFE proved highly efficient for the Li-S cell. The first discharge in either ACN:HFE (1:1) or ACN:HFE (1:2) (see **Figure 1a**) exhibits a high capacity (1373 mAh $g^{-1}$ and 1170 mAh $g^{-1}$, respectively) indicating a higher sulphur utilization via the decrease in viscosity (**Figure S2**). Both ACN:HFE blends exhibit a higher specific capacity after 100 cycles than DOL:DME (1:1) – 850 mAh $g^{-1}$ and 724 mAh $g^{-1}$ vs. 694 mAh $g^{-1}$, respectively (**Figure 1c**). Among the two, ACN:HFE (1:1) benefits from a slightly higher molar ionic conductivity, which results in the best electrochemical performance. Notably, the addition of HFE to $(ACN)_2$:LiTFSI did not alter the sloping feature of the voltage profile, nor the absence of supersaturation (**Figure 1a,b**). Again, we believe that the immobility of polysulphide species is responsible for this unique behaviour. The excellent coulombic efficiency is also maintained (**Figure 1c**), without the need for any $LiNO_3$ additive to passivate the negative electrode[7]. This is corroborated by the absence of coloration in the separator at any state of discharge (see **Figure S4**). Unlike polymer electrolytes[28] or even pure $(ACN)_2$:LiTFSI, where the viscosity results in a diffusion barrier, the excellent retention of polysulphides within the positive electrode for ACN:HFE electrolytes is attributed to their unique solvation inability, which in turn results in a unique electrochemical signature as discussed in the following section.

In contrast to catholyte cells that rely on full dissolution of polysulphides in electrolytes such as DOL:DME and hence usually exhibit excellent rate capability and energy efficiency[29,30] - with the detriment of low volumetric capacity - restricting polysulphide solubility with this approach results in an expected increase in cell polarization.

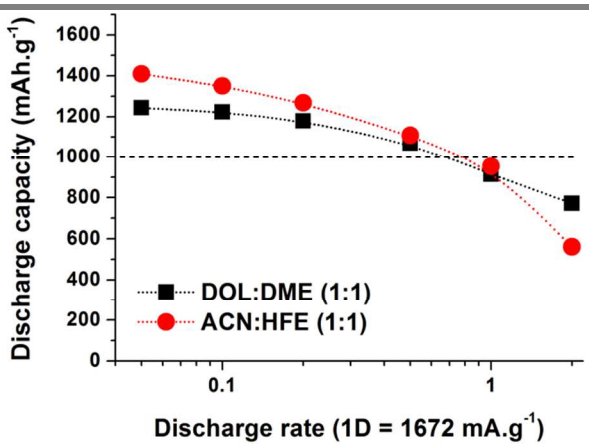


**Figure 2**. Ragone plot showing ACN:HFE (1:1) (red) outperforms DOL:DME (black) at discharge rates up to 1C. Measured on 2nd discharge, after a formation cycle at C/10.

Energy & Environmental Science
View Article Online
DOI: 10.1039/C4EE00372A ARTICLE



Remarkably though, the power performance of ACN:HFE (1:1) exceeds that of DOL:DME at rates of 1C and lower, with a discharge capacity of 900 mAh $g^{-1}$ at 1C. **(Figure 2)**. To the best of our knowledge, this result is more than four-fold superior to that previously reported RTILs for Li-S[17,20,23]. The high concentration in LiTFSI (1.8 M), associated with the suitable viscosity discussed above provide a sufficient reservoir of $Li^+$ at the sulphur electrode surface so that low mobility of polysulphides is not an impediment to reach practical current rates.

**Sulphur reduction mechanism in ACN:HFE electrolytes.**

From the galvanostatic cycling data alone, we cannot determine whether polysulphides are not formed in $(ACN)_2$:LiTFSI - as was suggested for other glyme-based RTILs [20,23] - but just that their solubility and mobility within the electrolyte is negligible. A simple colorimetric experiment that proves this point is presented in **Figure 3**. Sulphur electrodes that were partially discharged *vs.* lithium in ACN:HFE (1:1) were recovered and soaked in TEGDME. While the original ACN:HFE (1:1) solution was completely colourless, TEGDME immediately turned colour upon polysulphide extraction from a partially discharged sulphur positive electrode. At 100 mAh $g^{-1}$ the solution was brown-red, but thereafter green. As reported in the literature, lithium polysulphides exhibit different colours in solution, from red to green and yellow for long, medium and short chains, respectively[31,32]. Hence, we propose the formation of polysulphide intermediates on discharge rather than a biphasic reduction of sulphur to $Li_2S$. This visual test indicates a decrease in the average chain length after the upper discharge plateau at 2.2 V, while the emerald green color observed from then on suggests that medium chain polysulphides persist until the end of discharge, albeit in decreasing concentration. While the solubility of $Li_2S_2$ in glymes is still subjected to assumption[33], our experiment furthermore suggests that short chain polysulphides are either not present at the end of discharge or are poorly soluble in TEGDME.

In order to monitor the unique electrochemistry of sulphur in ACN-based electrolytes in real time, *operando* synchrotron XANES measurements at the sulphur K-edge were performed. Unfortunately, neither $(ACN)_2$:$LiClO_4$ nor $(ACN)_2$:$LiPF_6$ are liquid at room temperature[21] and thus TFSI is a vital component of the $(ACN)_2$:LiTFSI complex. Therefore, the sulphur K-edge spectra are dominated by the LiTFSI contribution around 2477 eV as shown in **Figure S5**. Nevertheless, the absorbance of the electrolyte remains constant upon cycling (as confirmed experimentally by the constant edge step) so that the LiTFSI component could be carefully subtracted from the spectra collected upon discharge, resulting in **Figure 4a** and **Figure 4c**.

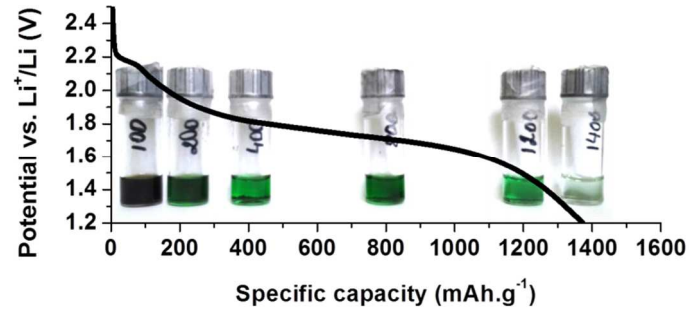


**Figure 3**. Pictures of electrodes partially discharged in ACN:HFE (1:1), and then extracted with TEGDME.

Compared to reference spectra (**Figure 4b**)[26], significant fluorescence distortion can be assessed from the examples of pristine and discharged states (**Figure 4c**). This distortion is nonlinear (high intensity features are more severely affected) so that a quantitative linear combination fitting[26] was not attempted. Nonetheless, the XANES spectra exhibit clear variations as a function of discharge capacity so that a qualitative data analysis is possible. Both the voltage profile and the specific discharge capacity at C/10 of 1380 mAh $g^{-1}$ are in good agreement with previous electrochemical studies (see **Figure 1**).

As recently confirmed by first principle calculations[34], the low energy feature around 2468 eV observed in $S_6^{2-}$ or $S_2^{2-}$ (**Figure 4b**) is characteristic of chain polysulphides[9,26]. The appearance and increase in intensity of this feature upon discharge thus confirms the progressive formation of polysulphide intermediates in the ACN-based electrolyte as discussed above. The persistence of pale coloration in the ether-extracted electrode at 1400 mAh $g^{-1}$ shown in **Figure 3** – indicating the presence of a low concentration of polysulphides – is also supported by XANES that shows persistence of the low energy feature at the end of discharge (**Figure 4a** and **5c**).

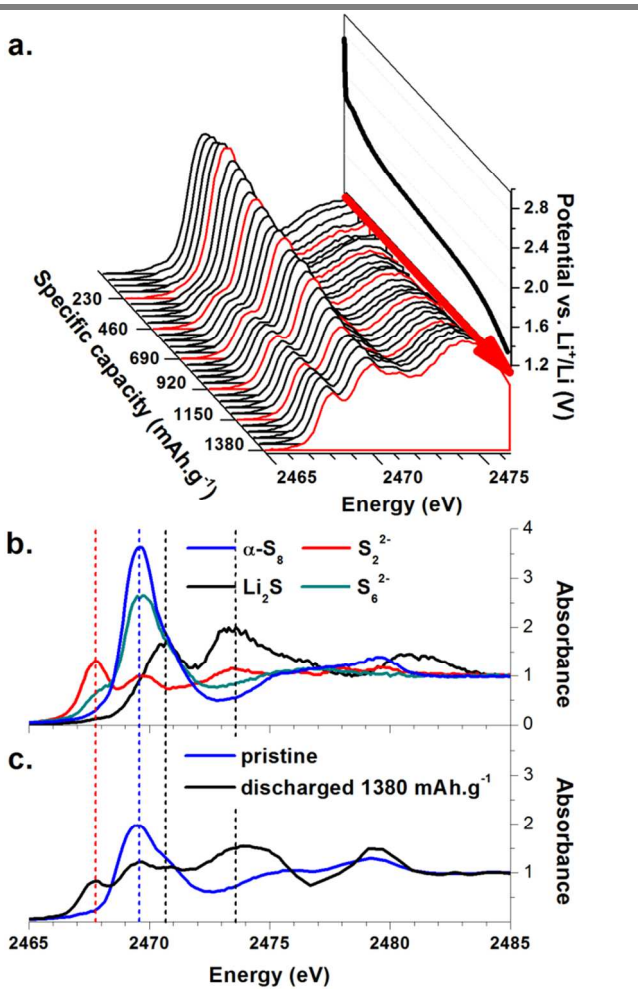


**Figure 4**. Sulphur K-edge XANES showing: **a.** Evolution of absorbance as a function of the electrochemical discharge at C/10. **b.** Reference spectra for elemental sulphur (blue), $S_2^{2-}$ (red) and $Li_2S$ (black). **c.** Pristine (blue) and discharge state (black). Dotted lines highlight the contribution of the difference reference species to the spectra acquired *operando*.

View Article Online
Energy & Environmental Science
DOI: 10.1039/C4EE00972A



Both imply the incomplete reduction of sulphur in ACN:HFE (1:1) to a mixture of short polysulphides and $Li_2S$ (**Figure 4b**). The variation in absorbance as a function of discharge capacity is plotted in **Figure 5b** and profiles at 2467.8 eV (low energy), 2469.5 eV (white-line) and 2474 eV ($Li_2S$) are given in **Figure 5c** to facilitate the comparison with sulphur redox in a conventional DOL:DME (1:1) electrolyte[26]. Remarkably, the variations in the electrochemical discharge potential **(Figure 5a**) are well reflected in the XANES spectra and in the low energy feature in particular.

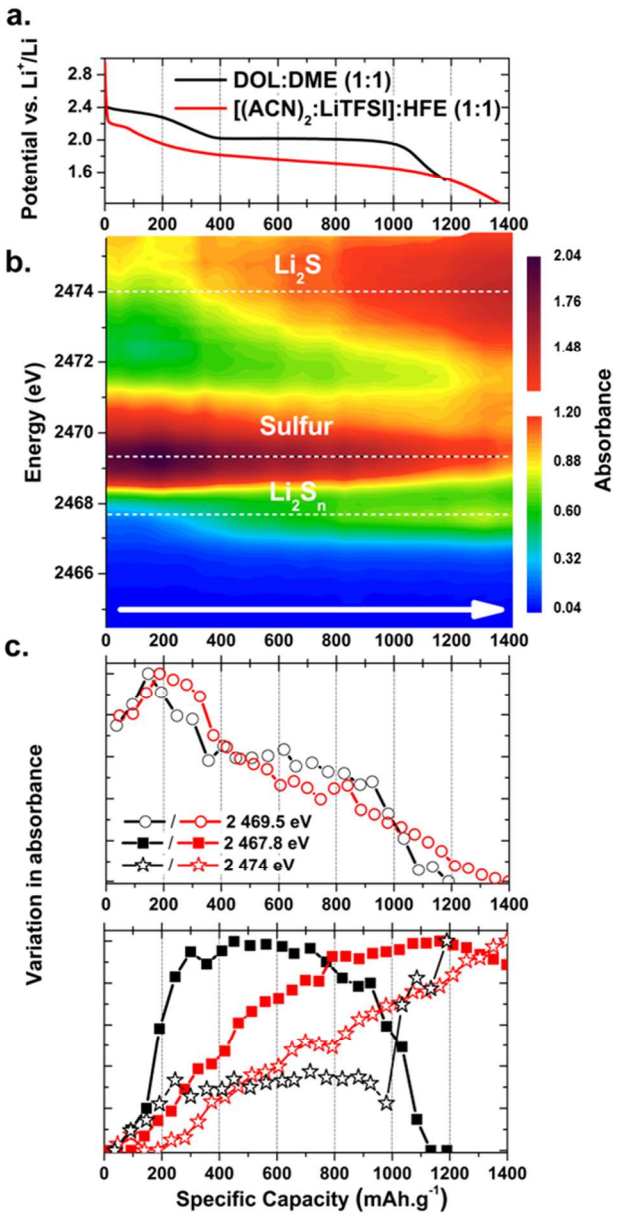


**Figure 5**. Comparison of DOL:DME (1:1) and ACN:HFE (1:1) electrolyte by operando sulphur K-edge XANES. **a.** Voltage profile upon reduction at C/10. **b.** Variation of the fluorescence upon reduction for ACN:HFE (1:1). Dotted lines mark the energies indicative of linear polysulphides (low energy, 2468 eV), sulphur white-line (2469.8 eV) and $Li_2S$ (2474 eV). These three slices are reported in **c.** (red) and compared to the case of DOL:DME (1:1) (black).

In DOL:DME (1:1), the two phase transitions, solid → solution followed by solution → solid, are manifested by a sudden increase, or drop in the intensity of the low energy feature characteristic of chain polysulphides, respectively. In contrast, in ACN:HFE (1:1), the smooth and sloping discharge curve translates into a linear increase of this low energy feature on the sulphur K-edge to reach a maximum at a capacity of 840 mAh $g^{-1}$. As previously demonstrated[26,34], lithium polysulphides all exhibit the same XANES features (both a low energy and the white-line peak); only the relative intensity of these two peaks varies inversely with the variation in of the polysulphide chain length. Therefore, the simultaneous increase of the low energy and decrease of the white line observed in **Figure 5b** and **Figure 5c** for ACN:HFE (1:1) can be interpreted as a gradual shortening of the $S_n^{2-}$ chains, typically from n = 8 to n = 2. The fact that the low energy feature starts diminishing at the end of discharge, together with the simultaneous decrease of the white-line, and increase at 2471 eV and 2474 eV (**Figure 5b**), suggests the conversion of polysulphides to $Li_2S$. Interestingly, the spectral feature at 2474 eV characteristic of $Li_2S$ increases linearly after 320 mAh $g^{-1}$ (**Figure 5c**), implying that $Li_2S$ is formed early and progressively in the discharge process. **Figure 5c** shows that in DOL:DME (1:1), the polysulphide concentration reaches a maximum around 400 mAh $g^{-1}$, whereas the signature of $Li_2S$ is absent until further along in the plateau. By contrast, in ACN:HFE (1:1), the fraction of polysulphide remains low due to the very limited fraction of "free" ACN available for solvation, and hence conversion to $Li_2S$ immediately triggers precipitation. In this respect, the overpotential (see **Figure 1a,b** and **Figure 5a)** can be understood as the result of the slower kinetics for polysulphide solvation in ACN:HFE (1:1) compared to DOL:DME (1:1), while the sloping discharge profile reflects the precipitation of $Li_2S$ within a gradually more reduced solution.

In order to confirm the origin of the overpotential in ACN:HFE (1:1), and further investigate its implications, we relied upon classical electrochemical titration methods that provide a probe of the Li-S system at close to thermodynamic equilibrium. Unfortunately, the time constraints associated with these experiments is incompatible with a XANES synchrotron run. **Figure 6** shows the chronoamperograms obtained from staircase voltammetry. The voltage was stepped sequentially and the current was monitored until it reached a predetermined Imin minimum value (see Experimental). From the incremental capacity curves (**Figure 6b**), it is easy to discern the "high voltage" peak corresponding to reduction of elemental sulphur to long chain polysulphides, polarized from 2.4 V in DOL:DME (1:1) to 2.2 V in ACN:HFE (1:1) as a result of the overpotential. The capacity integrated on this peak can be doubled in ACN:HFE (1:1) by lowering $I_{min}$ from C/50 (red curve) to C/100 (see SI, **Figure S6**), implying the kinetics of this reaction is extremely slow compared to DOL:DME (1:1). This can explain why it is not observed at all in pure $(ACN)_2$:LiTFSI, and the cell then polarizes down to the "low voltage" region. For both electrolytes, the onset voltage for the reduction of polysulphides to $Li_2S$ is about 2.1 V; however the chronoamperograms are drastically different. For the cell run in DOL:DME (1:1) (black curve), the current response is extremely high in a narrow potential window. It exhibits the typical signature of a biphasic reaction where the potential is incremental before the end of the phase transition (**Figure 6a**).

Energy & Environmental Science
View Article Online
DOI: 10.1039/C4EE00372A ARTICLE



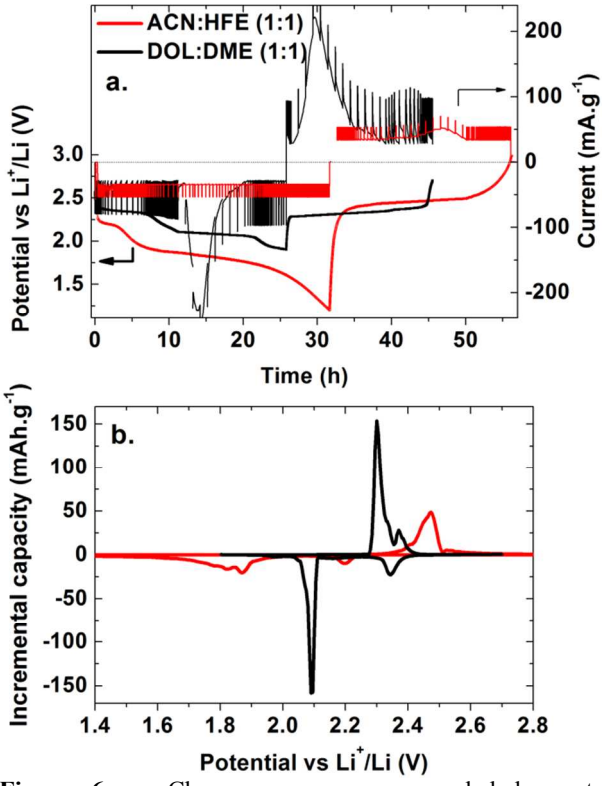


**Figure 6**. **a.** Chronoamperograms recorded by potential staircase voltammetry in DOL:DME (1:1) (black) and ACN:HFE (1:1) (red). Steps are set to 5 mV $h^{-1}$ with a C/50 current limitation. **b.** Incremental capacities obtained by integrating current over each potential step.

For the cell run in ACN:HFE (1:1), the current remains extremely low over the reduction of polysulphides to $Li_2S$ over a wide voltage window, and only a lower current limit ($I_{min}$ = C/100, **Figure S6**) allows the observation of the signature of a biphasic reaction. The implication is that $Li_2S$ nucleation in ACN:HFE (1:1) is controlled by the slow kinetics for polysulphide diffusion and/or lithium (de)solvation from $(ACN)_2$:LiTFSI. It therefore proceeds in a more incremental manner than in DOL:DME (1:1), where rapid (anti)dismutation equilibria govern the distribution of sulphur species[31]. On the macroscale, we propose that it is likely that the low mobility in ACN:HFE (1:1) keeps polysulphides species in close contact with the conductive host, thus preventing the aggregation of $Li_2S$ and loss of electronic contact. Lastly, the comparison of the incremental charge and discharge capacities (**Figure 6b**) indicates that in both electrolytes, sulphur redox is perfectly reversible. The onset oxidation voltage is about 2.25 V where the kinetic limitation arising from (de)solvation polarizes this process in ACN:HFE (1:1).

To confirm that chemical equilibria in a Li-S cell can indeed be overruled by a specifically targeted electrolyte formulation, we performed galvanostatic intermittent titration experiments (GITT). Here, constant current is delivered in short pulses, and the system is allowed to relax to equilibrium (see Experimental). **Figure 7a** shows a GITT experiment conducted in ACN:HFE (1:1). Remarkably, the voltage-composition profile representing a state of electrochemical equilibration (quasi OCV; shown by the red line) resembles the more typical behavior of sulphur in DOL:DME (1:1), shown in **Figure 7b**. A major difference with common electrolytes or previously reported RTILs is that in our case, theoretical discharge capacity can be achieved reversibly (the second discharge reaches 1400 mAh $g^{-1}$), even without positive electrode optimization. This indicates that electronic conductivity is not the limiting parameter in the Li-S cell under these quasi-equilibrium conditions, providing $Li_2S$ precipitation can be kinetically controlled. The close-to-theoretical capacity on first discharge suggests that mechanisms that we have previously reported which account for limited capacity in DOL:DME (1:1) (namely, the faster kinetics of reduction of polysulphides *vis a vis* sulphur formed via disproportionation)[26] are not operative in the ACN:HFE electrolyte. We believe this is due to suppression of the $S_8^{2-} \rightarrow$ ¼ $S_8$ + $S_6^{2-}$ disproportionation reaction[31], which requires mobility of solvated $S_8^{2-}$ in significant concentrations. Between the current pulses and the rest periods, we note an overpotential of about 200 mV on discharge and a comparable (even increasing) polarization in charge (**Figure 8a),** indicative of a kinetic limitation.

Difficulty in stripping and plating lithium from $(ACN)_2$:LiTFSI) at the negative electrode could be ruled out *via* a control GITT experiment in a 3-electrode cell, showing that the potential of the lithium counter electrode remains below 20 mV throughout (SI, **Figure S7**). This confirms that the kinetic limitation arises from the limited availability/mobility of sulphur redox species for the electrochemical reaction to proceed at the positive electrode. During discharge, ACN molecules released at the cathode ($Li^+$ desolvation) only have two options: complex with 1) LiTFSI or 2) with $Li_2S_n$. Conventional $Li^+$ solvation is excluded in superconcentrated solution[22]. If a $[(ACN)_2Li]_2S_n$ complex were to exist, its transport in solution would be equally negligible as solid $Li_2S_n$, owing to the absence of free solvent.

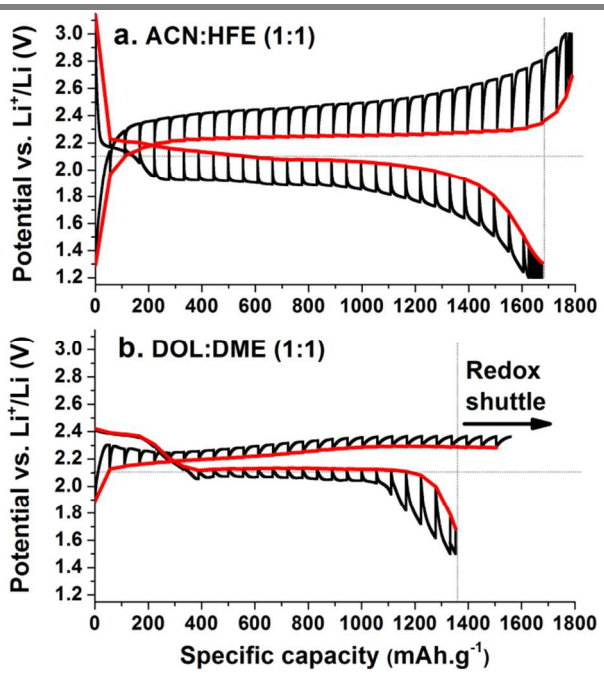


**Figure 7**. GITT experiments in **a.** ACN:HFE (1:1) and **b.** DOL:DME (1:1) without $LiNO_3$ additive. Curve in red is constructed from the last data point of each OCV period. The vertical dashed lines highlight the overcharge ascribed to redox shuttle; the horizontal dashed line highlights that the equilibrium reduction potential in ACN:HFE (1:1) decreases all along discharge.

View Article Online
Energy & Environmental Science
DOI: 10.1039/C4EE00372A



The consequence is a somewhat higher polarization between charge and discharge and a sloping voltage profile: characteristic proof of polysulphide insolubility. Such systems are not limited to $(ACN)_2$:LiTFSI electrolytes, and provide an opposite approach to that used in low volumetric energy density catholyte cells.

The good interfacial properties towards lithium observed at C/10 (**Figure S7**), means that the cycle life and safety of a Li-S battery incorporating ACN:HFE electrolyte can be greatly extended by using a low charging current rate ($\leq$ C/10) to prevent parasitic reactions that occur when the $Li^+$ diffusion within the electrolytes is slower than lithium desolvation from the complex. Thus, the rate of fading is directly related to the charge rate. This can be observed in **Figure 8**, where comparison of the same discharge/charge rate couples (i.e. D/10–C/10 to D/2–C/2, open symbols) shows that fading is aggravated at the faster rates. At the same discharge rate of D/5, charge at C/10 significantly reduces fade vs C/5 (red symbols). Capitalizing on this knowledge results in capacities of 1000 mAh $g^{-1}$ at D/2 that exhibit very little capacity fade. We anticipate that a Li metal electrode prevented from direct contact with the "free" acetonitrile in the electrolyte by a protective film could be used in practical cells for long term cycling. Perhaps even more promising, the excellent behaviour of $(ACN)_2$:LiTFSI at the interface with graphite in a Li-ion cell was recently demonstrated by Yamada *et al.*[22]. The insolubility of polysulphides in the electrolyte furthermore allows the freedom of designing Li-ion sulphur batteries.

## Conclusions

The spectroscopic and electrochemical evidence presented here clearly demonstrates that polysulphide intermediates are formed in the $(ACN)_2$:LiTFSI -HFE electrolytes despite their very limited solubility for these species. Parasitic disproportionation reactions in the Li-S cell are potentially suppressed owing to the activated process necessary for decomplexation of solvent from $(ACN)_2$:LiTFSI, which limits the solvation and mobility of the polysulphides. As a result, $Li_2S$ is detected earlier and its formation proceeds more smoothly along the discharge process compared to the common DOL:DME electrolyte, so that the theoretical capacity can be reached. At practical cycling rates, the migration of polysulphides away from the positive electrode is prevented, which results not only in excellent coulombic efficiency but also improved capacity retention.

The chemical immobilization of sulphur species renders the use of physical confinement unnecessary, and preliminary experiments suggest that very good capacities are obtainable up to a C/5 rate with a commercial carbon black. However, electronic conductivity becomes even more critical when the active sulphur mass is rendered immobile. In short, this approach shows the way forward to increase the electrode sulphur loading by developing electrode architectures with open porosity but without risk of polysulphide dissolution. It should inspire the discovery of new electrolytes that exhibit the same behaviour but with greater intrinsic stability toward metallic lithium.

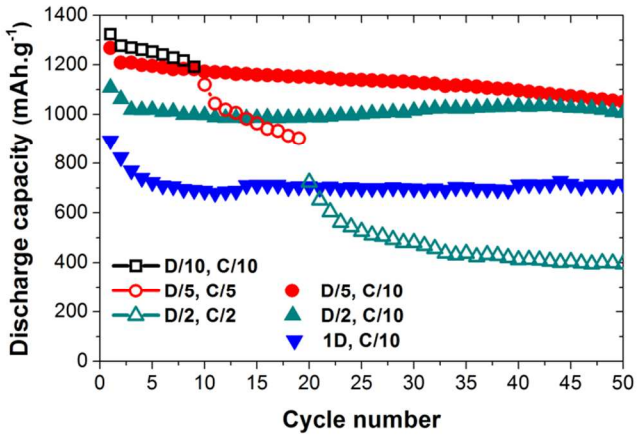


**Figure 8**. Galvanostatic experiments at matching charge rates (open symbols) vs. slow charge rate (C/10, full symbols) at D/5 (red), D/2 (teal) and 1D (blue) in ACN:HFE (1:1).

## Acknowledgements

The research was supported by the BASF International Scientific Network for Electrochemistry and Batteries. Use of the Advanced Photon Source (APS) was supported by the U. S. Department of Energy, Office of Science, Office of Basic Energy Sciences, under contract No DE-AC02-06CH11357. We thank Dr. T. Bolin for helping with the acquisition of the XANES data at the APS.

## Notes and references

[a] Department of Chemistry, Waterloo Institute for Nanotechnology, University of Waterloo, 200 University Ave W, Waterloo, Ontario N2L 3G1, Canada

[b] BASF SE, Ludwigshafen, 67056 Germany

[c] X-ray Science Division, Argonne National Laboratory, Argonne, IL-60439, USA

Electronic Supplementary Information (ESI) available: Physico-chemical characterization of LiTSI and $Li_2S_6$-saturated HFE, EIS equivalent circuit and fitted parameters, photographs of separators recovered at different states of discharge, details on the LiTFSI correction applied to XANES spectra, additional PITT and 3-electrodes GITT curves.

1 H. Yamin, A. Gorenshtein, J. Penciner, Y. Sternberg, and E. Peled, *J. Electrochem. Soc.,* 1988, **133**, 1045.

2 S.-E. Cheon, K.-S. Ko, J.-H. Cho, S.W. Kim, E. Y. Chin, and H.-T. Kim, *J. Electrochem. Soc.,* 2003, **150**, A796.

3 M.-K. Song, E. J. Cairns, and Y. Zhang, *Nanoscale*, 2013, **5**, 2186.

4 R. D. Rauh, K. M. Abraham, G. F. Pearson, J. K. Surprenant, and S. B. Brummer, *J. Electrochem. Soc.*, 1979, **126**, 523.

5 R. D. Rauh, F. S. Shuker, J. M. Marston, and S. B. Brummer, *J. Inorg. Nucl. Chem.*, 1977, **39**, 1761.

6 S.-E. Cheon, K.-S. Ko, J.-H. Cho, S.-W. Kim, E. Y. Chin, and H.-T. Kim, *J. Electrochem. Soc.*, 2003, **150**, A800.

7 D. Aurbach, E. Pollak, R. Elazari, G. Salitra, C. S. Kelley, and J. Affinito, *J. Electrochem. Soc.*, 2009, **156**, A694.

Energy & Environmental Science
View Article Online
DOI: 10.1039/C4EE00372A ARTICLE

8 J.-H. Song, J.-T. Yeon, J.-Y. Jang, J.-G. Han, S.-M. Lee, and N.-S. Choi, *J. Electrochem. Soc.*, 2013, **160**, A873.
9 J. Gao, M. A. Lowe, Y. Kiya, and H. D. Abruña, *J. Phys. Chem. C*, 2011, **115**, 25132.
10 T. Yim, M.-S. Park, J.-S. Yu, K. J. Kim, K. Y. Im, J.-H. Kim, G. Jeong, Y. N. Jo, S.-G. Woo, K. S. Kang, I. Lee, and Y.-J. Kim, *Electrochimica Acta*, 2013, **107**, 454.
11 E. Peled, Y. Sternberg, A. Gorenshtein, and Y. Lavi, *J. Electrochem. Soc.*, 1989, **136**, 1621.
12 D.-R. Chang, S.-H. Lee, S.-W. Kim, and H.-T. Kim, *J. Power Sources*, 2002, **112**, 452.
13 C. Barchasz, J.-C. Leprêtre, S. Patoux, and F. Alloin, *J. Electrochem. Soc.*, 2013, **160**, A430.
14 M. K. Song, Y. G. Zhang, and E. J. Cairns, *Nano Letters*, 2013, **13**, 5891.
15 T. Tamura, T. Hachida, K. Yoshida, N. Tachikawa, K. Dokko, and M. Watanabe, *J. Power Sources*, 2010, **195**, 6095.
16 W. Henderson, *J. Phys. Chem. B.*, 2006, **110**, 13177.
17 N. Tachikawa, K. Yamauchi, E. Takashima, J.-W. Park, K. Dokko, and M. Watanabe, *Chem. Commun.*, 2011, **47**, 8157.
18 L. Suo, Y. S. Hu, H. Li, M. Armand, and L. Chen, *Nat. Commun.*, 2013, **4**, 1481.
19 Y. Zhang, S. Liu, G. Li, G. Li, and X. Gao, *J. Mater. Chem. A*, 2014, DOI: 10.1039/C3TA14914E
20 J.-W. Park, K. Yamauchi, E. Takashima, N. Tachikawa, K. Ueno, K. Dokko, and M. Watanabe, *J. Phys. Chem. C*, 2013, **117**, 4431.
21 D. M. Seo, O. Borodin, S.-D. Han, P. D. Boyleand W. A. Henderson. *J. Electrochem. Soc.*, 2012, **159**, A1489.
22 Y. Yamada, K. Furukawa, K. Sodeyama, K. Kikuchi, M. Yaegashi, Y. Tateyama, and A. Yamada, *J. Am. Chem. Soc*, 2014, **136**, 5039.
23 K. Dokko, N. Tachikawa, K. Yamauchi, M. Tsuchiya, A. Yamazaki, E. Takashima, J.-W. Park, K. Ueno, S. Seki, N. Serizawa and M. Watanabe, *J. Electrochem. Soc*., 2013, **160**, A1304.
24 W. Weng, V. G. Pol, and K. Amine, *Advanced Materials*, 2013, **25**, 1608.
25 X. Ji, K. T. Lee, and L. F. Nazar, *Nat. Mater.*, 2009, **8**, 500.
26 M. Cuisinier, P.-E. Cabelguen, S. Evers, G. He, M. Kolbeck, A. Garsuch, T. Bolin, M. Balasubramanian, and L. F. Nazar, *J. Phys. Chem. Lett.*, 2013, **4**, 3227.
27 S. Z. Zhang, *J. Electrochem. Soc.*, 2012, **159**, A920.
28 D. Marmorstein, T. H. Yu, K. A. Striebel, F. R. McLarnon, J. Hou, and E. J. Cairns, *J. Power Sources*, 2000, **89**, 219.
29 J. R. Akridge, Y. V. Mikhaylik, and N. White. *Solid State Ionics*, 2004, **175**, 243.
30 Y. S. Su, Y. Fu, B. Guo, S. Dai, and A. Manthiram, *Chem Eur. J.*, 2013, **19**, 8621.
31 C. Barchasz, F. Molton, C. Duboc, J.-C. Leprêtre, S. Patoux, and F. Alloin, *J. Anal. Chem.*, 2012, **84**, 3973.
32 Y. Li, H. Zhan, S. Liu, K. Huang, and Y. Zhou, *J. Power Sources*, 2010, **195**, 2945.
33 K. Kumaresan, Y. Mikhaylik, and R. E. White, *J. Electrochem. Soc.*, 2008, **155**, A576.
34 T. A. Pascal, K. H. Wujcik, J. Velasco-Velez, C. Wu, A. A. Teran, M. Kapilashrami, J. Cabana, J. Guo, M. Salmeron, N. Balsara and D. Prendergast, *J. Phys. Chem. Lett.*, 2014, **5**, 1547.

## Table of Content Figure

An approach to new electrolyte systems for the Li-S battery, based on nonsolvents for polysulphides, enables high reversible capacities at very suitable rates and provides an improved fundamental understanding.